International Journal of Cardiology Cardiovascular Risk and Prevention 26 (2025) 200443

Contents lists available at ScienceDirect

International Journal of Cardiology Cardiovascular Risk and Prevention

journal homepage: www.journals.elsevier.com/international-journal-of-cardiology-cardiovascular-risk-and-prevention

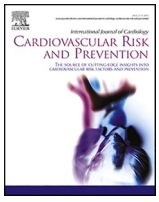

S100A4-shRNA mitigates autophagy, reduces inflammation, and improves cardiac functionality in MIRI

Guangwei Huang [a,b,*,1], Qing Huang [a,1], Chenrui Mou [c], Anna Duan [a], Fujiao He [b], Hailong Dai [b,**]

[a] Department of Cardiovascular Medicine, Anshun City People's Hospital, Anshun, 561000, Guizhou, China
[b] Department of Cardiology, Key Laboratory of Cardiovascular Disease of Yunnan Province, Yan'an Affiliated Hospital of Kunming Medical University, China
[c] The Third Affiliated Hospital of Kunming Medical University, Kunming, 650100, Yunnan, China

ARTICLE INFO

Handling editor: D Levy

Keywords:
S100A4
Reperfusion-injury
Autophagy
Inflammation

ABSTRACT

Background: S100A4 plays a crucial role in myocardial ischemia-reperfusion injury (MIRI), where the interplay between autophagy and inflammation shapes the progression of reperfusion injury. However, the specific mechanisms by which S100A4 influences autophagy and inflammation in this context remain unclear.
Methods: An ischemia-reperfusion (I/R) model was established in mice. The optimal timing for inducing reperfusion injury was determined, and mice were divided into sham and experimental groups. The experimental group underwent 2 h of ischemia/reperfusion injury followed by a 2-day reperfusion period. In the I/R + S100A4-shRNA group, S100A4 silencing was achieved through the injection of short hairpin RNA (shRNA). Myocardial ischemia was induced by occluding the left anterior descending branch (LAD) of the coronary artery. Diagnostic procedures, including electrocardiogram assessments, cardiac function testing, cardiac enzyme analyses, and 2,3,5-triphenyl tetrazolium chloride (TTC) staining, were performed to assess myocardial injury. Immunohistochemistry, immunofluorescence staining, hematoxylin-eosin (HE) staining, and Masson trichrome staining were used to evaluate the expression levels of IL-1, TNF-a, morphological changes in cardiomyocytes, and cardiac fibrosis. Protein blotting was conducted to examine autophagy-related proteins and Bnip3 signaling-related proteins.
Results: The study showed an increase in S100A4 expression, as well as upregulation of autophagy orchestrating proteins (Beclin-1 and LC3), contributing to myocardial injury and expansion of myocardial infarction (MI). S100A4 played a multifaceted role by regulating autophagy through the BNIP3 pathway in MIRI. Silencing S100A4 resulted in reduced autophagy and inflammation, leading to decreased infarct size and improved cardiac function.
Conclusions: S100A4 is upregulated during MIRI and orchestrates autophagy through the BNIP3 pathway, influencing the progression of reperfusion injury following myocardial infarction. Inhibition of autophagy and mitigation of inflammatory responses by S100A4-shRNA provide protection against the detrimental effects of IRI on the heart.

1. Background

Acute myocardial infarction (AMI) stands as the predominant catalyst of mortality within both urban and rural populations, as underscored by the 2018 data report [1]. At the epicenter of MI intervention lies the imperative for expeditiously unblocking occluded vasculature. Nonetheless, the act of vessel unblocking can unfurl dire ramifications, encompassing arrhythmia [2], sluggish reperfusion, and even fatality [3], ccasioned by cardiac rupture [4]. This phenomenon of myocardial ischemia-induced injury in the wake of reperfusion is encapsulated as MIRI [5].

The process of reperfusion injury entails a confluence of adverse responses, encompassing acidosis [6], calcium overload [7], and energy depletion [8], among others. This myocardial impairment precipitates

* Corresponding author. Anshun, Guizhou, 561000, China.
** Corresponding author. Kunming, 650051, China.
E-mail address: 419263483@qq.com (G. Huang).
[1] Guangwei Huang and Qing Huang are contributed equally to this work.

https://doi.org/10.1016/j.ijcrp.2025.200443
Received 2 May 2025; Received in revised form 27 May 2025; Accepted 29 May 2025
Available online 29 May 2025

the demise of cardiomyocytes [9].consequently leading to their fatality. Mitochondria, as the energy reservoirs that fuel cardiomyocyte vitality and sustain metabolic equilibrium, assume a pivotal role. Autophagy, in its capacity for the self-cleansing of impaired mitochondria [10], thus mitigates the extent of extrinsic harm and, in turn, attenuates reperfusion injury [11]. Within the realm of autophagy regulation, diverse pathways emerge, including the classical mitochondrial depolarizing PTEN induced putative kinase 1(Pink1)/Parkinson juvenile disease protein 2 (Parkin) pathway [12], as well as the new stereotaxic autophagy receptor FUN14 domain containing 1 (FUNDC1) molecule-mediated pathway [13]. This inquiry notably centers on the autophagic conduit steered by BNIP3, a proteinhailing from the Bcl-2 family that, since its discovery in 1994, has been recognized for its interactions with Bcl2 protein and adenovirus E1B19KD [14]. Early investigations unveiled a substantial surge in BNIP3 expression during MIRI in mice, a trend that endured within cardiomyocytes [15].

S100 calcium-binding A4 (S100A4) constitutes a calcium-bound protein intrinsic to cardiomyocytes, exerting its role in safeguarding these cells against further harm and necrotic processes [16,17]. Recent investigations have unveiled the multifaceted involvement of S100A4, encompassing cardiomyogenesis [18], growth promotion, and the instigation and invigoration of cardiomyocyte viability. Moreover, within the context of MI, S100A4 exhibits a notable upsurge in expression, thus potentially emerging as a fresh prognostic indicator for gauging the magnitude of myocardial infarction severity [19]. Studies have shown that silencing S100A4 may reduce the size of MI and reduce cardiac fibrosis [20]. This delineates a prospective therapeutic target for attenuating reperfusion injury subsequent to myocardial infarction, albeit necessitating further validation through subsequent cellular and animal assessments.

In the present study, we scrutinized S100A4 expression within mouse models of MI, effectuated S100A4 inhibition via shRNA, and unveiled the modus operandi of S100A4 within the BIP3 signaling cascade in vivo.

2. Materials and methods

2.1. Ethical approval

The study received approval from the Animal Experimentation Committee of Guizhou Anshun city people's hosptial's Institutional Review Board and was executed in alignment with the animal care and usage protocols established by Anshun city people's hosptial and Guizhou medical university. The research adhered to the 2013 amendments to the Declamiceion of Helsinki.

2.2. Animal

The Model Animal Research Center of Guizhou Medical University provided adult male C57/BL6 mice (8 weeks old) with a body weight ranging from 20 ± 5 g. Prior to the commencement of the study, the mice were maintained on a standard diet and subjected to a light/dark cycle of 12 h each, at room temperature, for a minimum of 10 days. Vital signs and cardiac performance were documented as the initial step.

2.3. Research plan

To determine the optimal reperfusion duration, forty-two mice were initially randomized into seven groups: a sham group and six I/R groups with reperfusion periods ranging from 2 h to 2 days (I/R 2h, 4h, 6h, 8h, 1d, and 2d). Based on the peak expression of injury-related markers, a 2-h ischemia followed by 2-day reperfusion protocol was selected for subsequent experiments.For the main experimental study, mice were randomly assigned into three groups:

(1) Sham group (mice underwent sham surgery and received a tail vein injection of non-targeting shRNA), (2) I/R group (mice subjected to I/R and injected with non-targeting shRNA), and (3) I/R + S100A4-shRNA group (mice subjected to I/R and injected with S100A4-targeting shRNA).

2.4. Preparing for surgery

After a week-long acclimation period, the animals underwent anesthesia via intraperitoneal injection of sodium pentobarbital at a dosage of 45 mg/kg. Following anesthesia, the toe-clamp test elicited no response, and trachea intubation ensued. Ventilator settings were harmonized with the anesthetized mice's respiratory rate, and the tracheal tube was linked to the ventilator. Preceding the surgical intervention, rat electrocardiograms were recorded utilizing a physiological signal acquisition and processing system. The thorax was accessed through the third intercostal space at the left sternum margin, where the LAD was ligated using a 7-0 silk suture. Thirty minutes later, the ligature was slackened to initiate reperfusion. Mice in the sham group were not subjected to treatment. Within this investigation, only the sham group underwent thoracotomy, with the LAD remaining unligated. The mice were positioned on a 30 °C warming pad with continuous postoperative cardiac monitoring for 10 min until reawakening. One week prior to modeling, mice in the Sham, IR and I/R + S100A4-shRNA groups were injected through the tail vein with either negative control (sh-NC) or S100A4-specific shRNA sequences (sh-S100A4). (Lentiviral plasmid 200 μL for 5×10^7TU/ml). (GenePharma, Shanghai, China).

2.5. CK-MB and cTnT evaluation

Cardiac troponin T (cTnT) and creatine kinase isoenzyme (CK-MB) were assayed to evaluate the extent of myocardial injury. As the endpoint of reperfusion time, blood collection is promptly initiated upon reaching the designated reperfusion time, and subjected to centrifugation at 1200 rpm for 10 min to procure plasma. Concentration of cTnT and activity of CK-MB were quantified employing ELISA assays (Quanzhou Ruixin Biological Technology Co., LTD, Quanzhou, China) as per the manufacturer's guidelines.

2.6. The chloride of triphenylterazolium (TTC) stains

TTC staining was used in mice heart tissue sections at 24 h after LAD occlusion and reperfusion. Mice myocardial tissue was excised and immersed in normal saline for 5 min. Sections with a thickness of 5 mm were meticulously sliced from the apex to the base of the heart, after which they were subjected to immersion in a 2 % solution of TTC. This solution was allowed to permeate the tissue for a period of 30 min while maintained at a temperature of 37 °C. Following this, a span of 48 h was dedicated to immersion in a 10 % formaldehyde solution. After staining, the infarcted area appeared as white, while normal heart tissue exhibited a red stain. Concluding this process, the slices were meticulously photographed, and the extent of the infarcted area was accurately calculated subsequent to comprehensive analysis. The results were determined by calculating the ratio of infarct size to the total size, multiplied by 100 %.

2.7. Staining with hematoxylin-eosin (HE)

Following the process of dewaxing, the myocardial section was meticulously sliced into sections measuring 3 μm in thickness. Hematoxylin staining solution was applied for a duration of 5 min, followed by a brief exposure to eosin staining lasting 10 s. Thorough washing ensued, with successive immersions in 85 % ethanol, 90 % ethanol, and anhydrous ethanol. A transparent eluent treatment was meticulously carried out, subsequently sealed with neutral resin. The ensuing

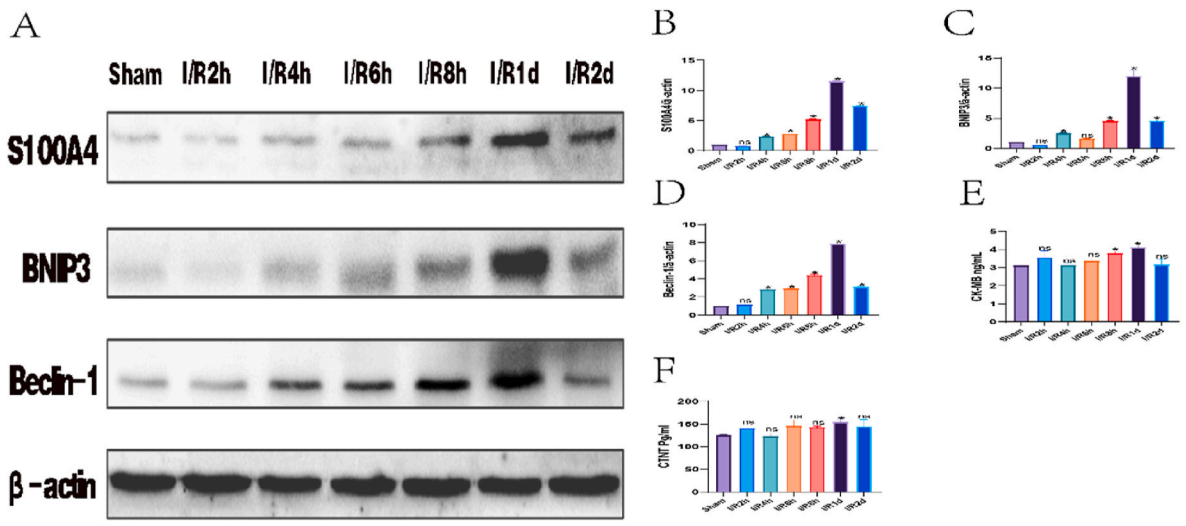

Fig. 1. Optimal time for reperfusion injury. (A–D) Western blotting was used to evaluate the levels of S100A4, BNIP3, and Beclin-1 in different treatment groups and quantitative analysis of bands. Values are expressed as mean ± SD. $^{*}p < 0.05$、$^{ns}P > 0.05$ vs sham group. (E–F) The cTnT content and activities of CK-MB were measured by ELISA.

observation and capture of images were executed using a sophisticated light microscope manufactured by Leica in Germany.

2.8. Immunohistochemistry

Employing deparaffinization and antigen retrieval techniques within a steam autoclave containing 1 mM EDTA (pH 8.0) for 16 min, the cardiac tissue was meticulously sectioned to a thickness of 5 m using paraffin. Subsequently, a 10 % goat serum was delicately applied, undergoing fixation through a water immersion at a temperature of 37 °C for a period of 45 min. This was succeeded by the meticulous application of appropriate primary antibodies at 4 °C over a span of 12 h, followed by the utilization of a general secondary antibody at ambient temperature for a duration of 30 min. In conclusion, hematoxylin was employed for nuclear staining, coupled with the application of a coloring agent to facilitate the observation of positive expression under a microscope.

2.9. Western blot analysis (WB)

WB analysis unveiled the presence of S100A4, BNIP3, Beclin-1, LC3, IL-1, and TNF proteins. For protein extraction, the Nuclear and Cytoplasmic protein extraction reagent (Yishan Biotech, Shanghai, China) was employed. Protein concentration was assessed using the BCA Protein Analysis Kit (Yishan Biotechnology). Subsequently, 50 g of protein were separated via 10 % SDS-PAGE and transferred onto polyvinylidene fluoride (PVDF) membranes from each extract. Notably, the following primary antibodies were employed: rabbit anti-BNIP3 (Abcam, China; 1:1000); rabbit anti-S100A4 (Abcam, China; 1:800); rabbit anti-Beclin-1 (Abcam, China; 1:1000); rabbit anti-LC3 (CST; USA; 1:1000); rabbit anti-IL-1 (CST; USA; 1:1000); rabbit anti-TNF (CST; USA; 1:800). After gentle flushing with Tris-buffer saline containing Tween, the membranes were incubated with goat anti-mouse or anti-rabbit IgG-HRP (1:6000; Santa; USA) and ECL reagent (Thermo; USA), with -actin serving as a pivotal endogenous control. The Optical Density of the bands was quantified using ImageProPlus 6.0 Analyzer Software.

2.10. Echocardiographic analysis

The study employed a Vivid 7 ultrasound system (GE, Horten, Norway) featuring an il3L intraoperative linear transducer operating at a frequency range of 11.0–15.0 MHz. A skilled operator conducted mouse imaging under gentle sedation, maintaining a controlled ambient temperature of 22–24 °C and minimizing extraneous lighting. M-mode parameters were acquired from the parasternal short-axis view, encompassing measurements such as left ventricular internal diameter at diastole (LVIDd), left ventricular internal diameter at systole (LVIDs), ejection fraction (EF), and fractional shortening (FS).

2.11. Statistical analysis

All experimental analyses, including infarct size quantification (TTC staining), echocardiographic measurements, enzyme-linked immunosorbent assays, and protein band intensity analysis, were performed by investigators who were blinded to the treatment group allocations. The experiments were performed in triplicate, and the results are presented as mean ± SD. Statistical differences between the groups were assessed using one-way analysis of variance (ANOVA), followed by the student–Newman–Keuls post hoc test. SPSS 26.0 software and GraphPad Prism were employed for all statistical analyses. A significance level of $p < 0.05$ was used to determine statistically significant differences.

3. Result

3.1. Basic characteristics

Random assignment of 60 male rodents to study groups and treatment protocols. In order to determine the optimal reperfusion time, 42 male mices were divided into 7 groups (sham, I/R 2h, I/R 4h, I/R 6h, I/R 8h, I/R 1d, I/R 2d groups) to detect the expression of S100A4, BNIP3 and Beclin-1 proteins and the altemiceions of myocardial enzymology. Then, 18 rodents were sepamiceed into three groups for verification purposes. None of the groups displayed a statistically significant difference in their vital baseline signs.

3.2. Optimal time for reperfusion injury

A substantial alteration was discerned in the protein expression patterns of S100A4, BNIP3, and Beclin-1 during the 2-h to 2-day timeframe (n = 6)(Fig. 1). Notably, the protein levels of S100A4, BNIP3, and Beclin-1 exhibited an ascending trajectory with the progression of reperfusion time, culminating on the initial day of reperfusion, followed by a subsequent decline ($P < 0.01$). The concentration profiles of CK-MB and cTnT, as depicted in Fig. 1A–D and 1E-F, respectively, mirrored this trend, reaching their zenith on the first day of reperfusion ($P = 0.006$),

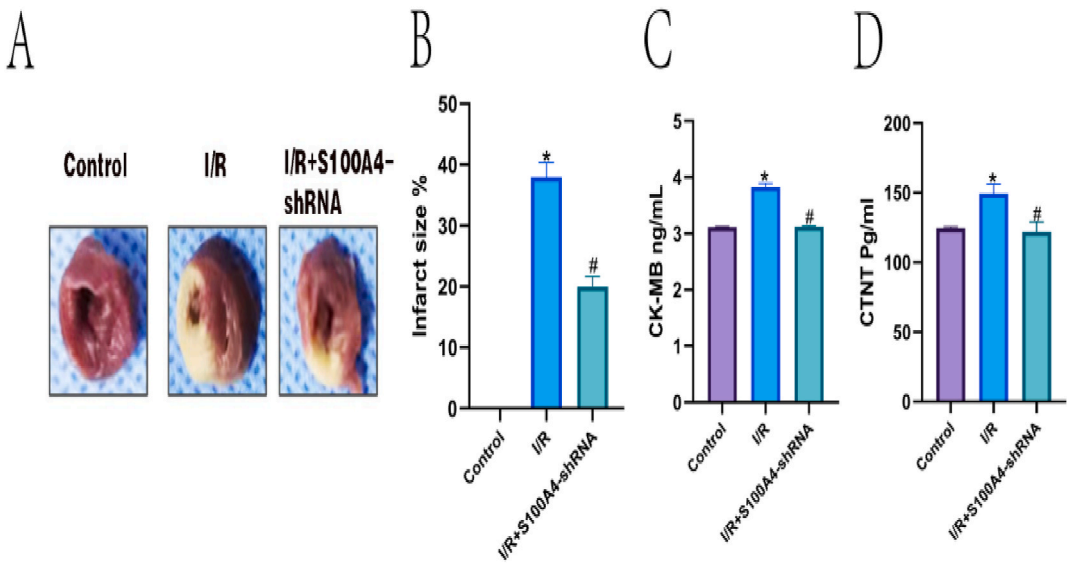

Fig. 2. S100A4-shRNA alleviates MIRI. (A–B) TTC staining was used to determine the magnitude of the infarct. The ischemic region appeared white, whereas the viable myocardium appeared red. As a proportion of the total segment area, the infarct area was quantified. Using TTC staining, the infarct area and viable myocardium were quantified (n = 4). (C–D) CK-MB and cTnT measured values and analysis by ELISA. A graphical representation of the infarct size as a percentage. $^{*}P < 0.05$ vs. the control group; $^{\#}P < 0.05$ vs. the I/R group. (For interpretation of the references to color in this figure legend, the reader is referred to the Web version of this article.)

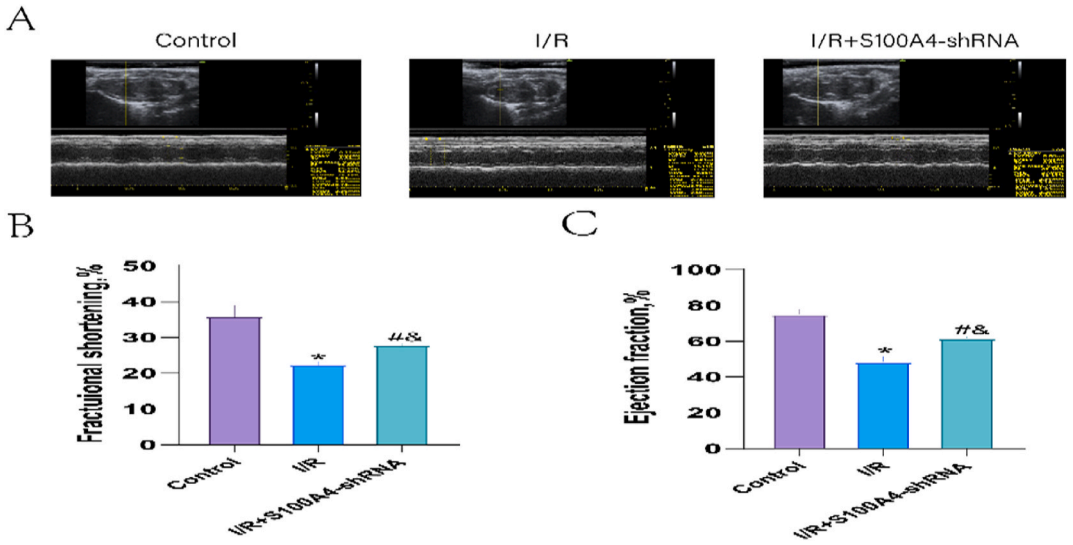

Fig. 3. S100A4-shRNA improve myocardial function after MIRI. (A) Representative echocardiogram after pretreatment with S100A4-shRNA after I/R injury (n = 4). (B–C) The proportion of EF and FS (n = 4). Data are expressed as mean ± SD. $^{*}P$、$^{\&}P < 0.05$ vs. the control group; $^{\#}P < 0.05$ vs. the I/R group.

thus establishing congruence with the observed protein expression pattern.

3.3. S100A4-shRNA alleviates MIRI

TTC staining unveiled a noteworthy diminishment in the MI region among mice subjected to S100A4-shRNA treatment ($P < 0.001$) (Fig. 2A–B). In contrast, in the I/R group, the concentrations of serum cTnT and CK-MB exhibited a marked elevation in comparison to the control group ($P = 0.004$ and $P < 0.001$), signifying pronounced myocardial impairment due to IR. Impressively, S100A4-shRNA administration strikingly countered this trajectory ($P = 0.003$ and $P < 0.001$) (Fig. 2C–D).

3.4. S100A4-shRNA improve myocardial function after MIRI

Relative to the control cohort, the I/R group demonstrated a noteworthy reduction in both FS and EF. Interestingly, the I/R + S100A4-shRNA intervention adeptly counteracted these alterations, leading to a marked enhancement in cardiac function ($P < 0.001$) (Fig. 3).

3.5. S100A4-shRNA inhibits autophagy via BNIP3 signaling pathway

Western blotting was used to ascertain the protein expressions of factors pertaining to the BNIP3 pathway and markers associated with autophagy. As illustrated in Fig. 4, the protein expressions of S100A4, BNIP3, and Beclin-1 within the I/R group exhibited a notable up-regulation, accompanied by a increase in the LC3-II/LC3-I ratio ($P < 0.01$). Intriguingly, administration of S100A4-shRNA led to a restoration

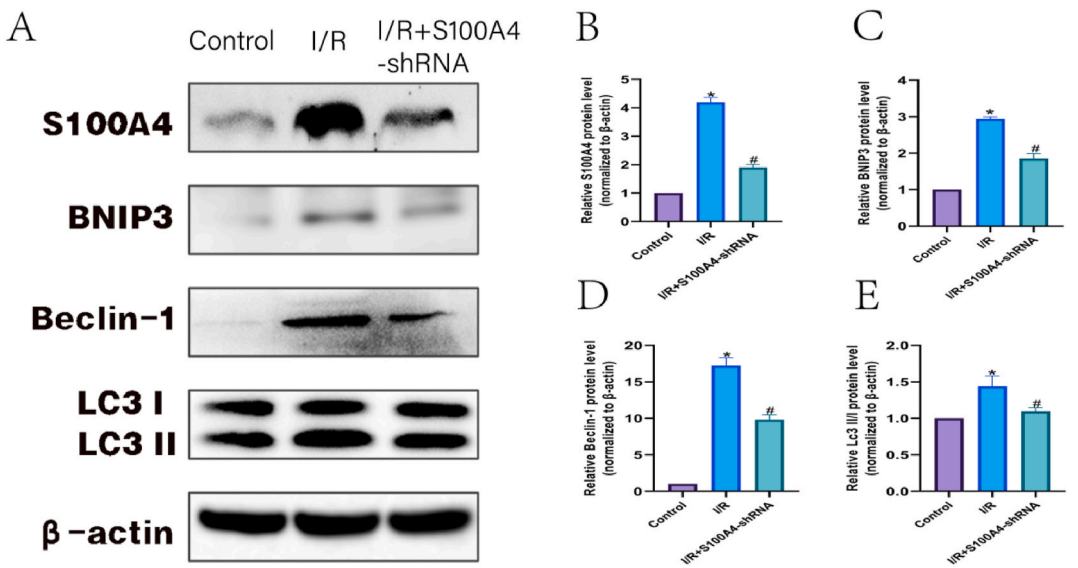

Fig. 4. S100A4-shRNA inhibits autophagy via BNIP3 signaling pathway. (A-E)The Western blot technique was employed to assess the protein expression levels of S100A4, BNIP3, Beclin-1, LC3 II/I, and β-actin in cardiac tissues from each experimental group. $^{*}P < 0.05$ vs. the control group; $^{\#}P < 0.05$ vs. the I/R group.

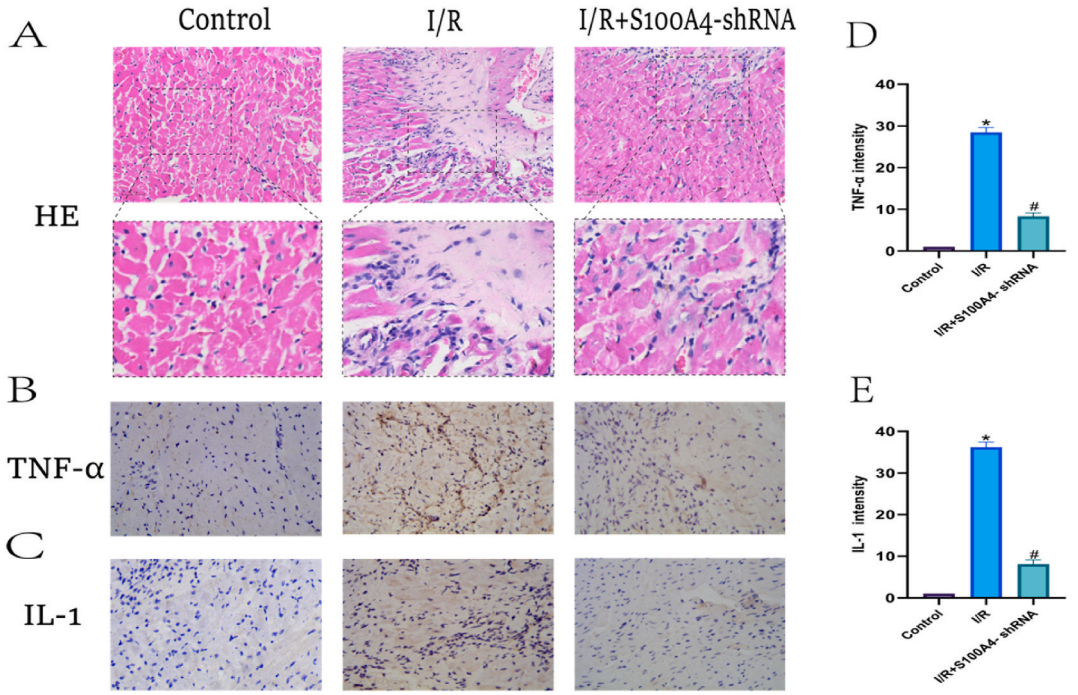

Fig. 5. S100A4-shRNA improve cardiomyocyte necrosis and inflammation. (A) H&E was utilized to assess the pathological and morphological altemiceions in the myocardial tissue. (B–E) The expression of IL-1 and TNF- in each of the three groups, as well as the miceios of their intensity measurementss. Scale bar: 50 μm; (n = 4). $^{*}P < 0.05$ vs. the control group; $^{\#}P < 0.05$ vs. the I/R group.

of protein expressions of S100A4, BNIP3, and Beclin-1 ($P < 0.001$). Compelling evidence underscores the role of S100A4 in stimulating the BNIP3 signaling cascade and augmenting autophagy.

3.6. S100A4-shRNA alleviates necrosis and inflammation in cardiomyocytes

H&E and IHC staining techniques were employed to scrutinize the morphological attributes and inflammatory status of myocardial cells in mice. As depicted in Fig. 5a, the control group manifested a well-ordered alignment of myocardial cells, featuring discernible nuclei and an absence of infiltrating inflammatory cells. Conversely, the I/R group displayed extensive myocardial tissue necrosis, accompanied by disrupted myocardial fiber arrangement and a substantial influx of inflammatory cells. Moreover, in the I/R group, there was a notable decrease in the count of myocardial cells. Contrastingly, within the I/R + S100A4-shRNA group, cellular disposition exhibited enhanced organization, while the severity and scope of cellular necrosis were notably mitigated. Notably, the expression levels of IL-1 and TNF-α were significantly augmented in the I/R group compared to the control group. Remarkably, administration of I/R + S100A4-shRNA evinced a substantial reduction in the expression of IL-1 and TNF-α ($P < 0.001$).

4. Discussion

The duration of IR displayed a discernible correlation with the expression of S100A4. Our observation revealed a zenith in expression after a single day of reperfusion, thereby establishing this timeframe as the point of origin for subsequent interventions. Upon the administration of S100A4-shRNA, we noted a reduction in autophagic activity compared to the I/R group. This attenuation contributed to ameliorated myocardial injury and enhanced cardiac function, thus thwarting reperfusion damage and safeguarding a larger complement of cardiomyocytes. These findings resonate with the research conducted by Gong et all [19], who underscored the substantial upregulation of S100A4 in response to I/R. The zenith of S100A4 expression and concurrent autophagy markers aligned with the reperfusion day, imparting a consistent trend. This alignment intimates that S100A4 potentially modulates reperfusion injury severity via autophagic modulation. Moreover, Shirin Doroudgar's findings illustrated that S100A4 abrogation exacerbated post-MI cardiac impairment. Conversely, targeted S100A4 overexpression in cardiomyocytes conferred protection upon the infarcted myocardium [21]. Animals deficient in S100A4 manifested compromised cardiac performance, coupled with heightened cardiac remodeling, fibrosis, and reduced myocardial capillary density distal to the affected region. However, Qian's research indicated that S100A4 gene knockout substantially curtailed cardiac fibrosis post-infarction in mice, suggesting the advantageous implications of S100A4 knockdown in the context of myocardial infarction. Our own findings complement this narrative by unveiling that the inhibition of S100A4 can mitigate IRI severity [22].

The role of autophagy in MIRI remains complex and context-dependent. Numerous studies have described autophagy as a double-edged sword, with moderate activation conferring protection during ischemia by clearing damaged organelles and preserving cellular homeostasis [23,24], whereas excessive or prolonged autophagy during reperfusion may exacerbate cell death and tissue damage [25]. In our study, S100A4-shRNA downregulated key autophagy-related proteins (BNIP3, Beclin-1, LC3-II/I) and simultaneously attenuated inflammatory cytokine expression (IL-1, TNF-α), indicating that inhibition of maladaptive autophagy may underlie its cardioprotective effects. Interestingly, the regulatory role of S100A4 in autophagy varies across tissues and disease models. For instance, Wei Shen et al. demonstrated that S100A4 depletion enhanced autophagy and differentiation in gastric cancer cells with mutant p53 [26], while Shasha Hou et al. reported that S100A4 promotes lung cancer progression by suppressing autophagy through the β-catenin/RAGE axis [27]. In contrast, Yulin Wang's study suggested that S100A4 inhibition facilitated corneal wound healing by promoting autophagy in alkali-burned rabbit corneas [28]. These divergent findings underscore the context-specific functions of S100A4 and suggest that its effect on autophagy is highly cell-type and environment dependent. In our cardiac model, the inhibition of S100A4 repressed excessive autophagic activity and alleviated inflammatory responses, supporting the notion that overactivation of autophagy during early reperfusion contributes to injury. This observation is consistent with recent studies highlighting the interconnection between autophagy and inflammation in MIRI pathophysiology [29]. Collectively, our results support a model in which S100A4 exacerbates MIRI by promoting maladaptive autophagy via the BNIP3 signaling pathway. Targeted inhibition of S100A4 may thus represent a therapeutic approach that tempers excessive autophagic activity while mitigating inflammation, ultimately preserving myocardial function after reperfusion.

Inflammation stands as a pivotal orchestrator of autophagy, where its fiery response assumes a guardianship role, invigorating cardiomyocyte autophagy during the nascent phase of MI. Notably, an independent inquiry corroborated this notion, suggesting that the early stages of myocardial infarction find solace in the protective embrace of the inflammatory response, thereby kindling cardiomyocyte autophagy's potential [30]. S100A4's intricate involvement extends its tendrils to an array of neuropathological processes, intricately shaping the fate of astrocytes, microglia, infiltrating cells, and neurons, thus adroitly modulating the symphony of inflammatory and immune responses within the neurorealm [31]. A discernible juncture materializes as S100A4 assumes the mantle of essential architect, choreographing the rapid assemblage of neutrophils following the MI's symphony [32].

Within our investigation, S100A4-shRNA elicited the quelling of early-stage inflammation and autophagy; nevertheless, the verdict on myocardial well-being remains inconclusive in the realm of early inflammation, while the interplay of early inflammation and autophagy potentially exerts sway over the panorama of ventricular remodeling post-infarction [33]. Demonstrating a pivotal role, S100A4-shRNA, orchestrating the modulation of autophagic evolution and confining the expanse of infarction, emerged as a linchpin, orchestrating the reduction in infarct dimensions and the enhancement of cardiac function through these empirical endeavors. Notably, in murine models, the attenuation of S100A4 has demonstrated the alleviation of cardiac fibrosis by way of the Wtn/-catenin pathway [22]. The temporal span of one reperfusion day failed to suffice for the discernment of myocardial fibrosis progression, thereby warranting the omission of staining methodologies like the Masson staining technique.

While our study demonstrates promising cardioprotective effects of S100A4-shRNA in a murine model of MIRI, several translational challenges must be considered before clinical application. One major concern is the delivery of RNAi therapeutics to the heart. In current cardiovascular research, AAV vectors and lipid nanoparticles (LNPs) are among the most commonly used carriers for RNA-based therapies, owing to their relative efficiency and tissue-targeting capabilities. However, AAV delivery may raise immunogenicity and integration concerns [34], while LNPs require optimization for cardiac tropism and systemic safety [35]. Another significant issue is the potential for off-target effects, which may lead to unintended gene silencing and toxicity. Advanced bioinformatics screening, in vitro specificity assays, and dose-controlled delivery strategies are critical to mitigate these risks. Notably, several preclinical studies have demonstrated the feasibility of cardiac-targeted RNAi therapy, and one siRNA-based drug (Inclisiran) targeting PCSK9 has already reached clinical use for cardiovascular indications, highlighting the translational potential of RNA-based approaches [36]. In future research, we will explore optimized delivery systems for S100A4-shRNA and systematically assess its tissue specificity, off-target profile, and long-term safety in larger animal models.

4.1. The limitations analysis

This experiment manifests a multitude of imperfections. Its validation solely remains confined to the realm of animal models and reductionist assays, leaving cellular validation conspicuously absent. Moreover, the substantiation of the direct pathway is notably wanting. Furthermore, the chosen reperfusion timeframe spanning 2 h to 2 days presents limitations hindering the comprehensive discernment of alterations in myocardial fibrosis and ventricular remodeling. Enhanced scrutiny and understanding can be garnered through the incorporation of pathway-specific inhibitors, along with the utilization of AC16 cardiomyocytes or primary cardiomyocytes for in vitro validation. Ferroptosis, a regulated form of cell death characterized by iron-dependent lipid peroxidation, has been increasingly recognized as a key contributor to myocardial ischemia-reperfusion injury (MIRI). Emerging studies suggest that ferroptosis not only aggravates reperfusion damage but also intersects with autophagy—particularly through ferritinophagy—and inflammatory signaling pathways [37,38]. Although our current study did not directly investigate ferroptosis, previous reports have shown that targeting ferroptosis-related pathways, such as ALOX15 activation or ferritin degradation, can attenuate ischemia-reperfusion injury [24,39]. Given that S100A4-shRNA treatment in our study led to reduced autophagy and inflammation, we speculate that S100A4 may also modulate

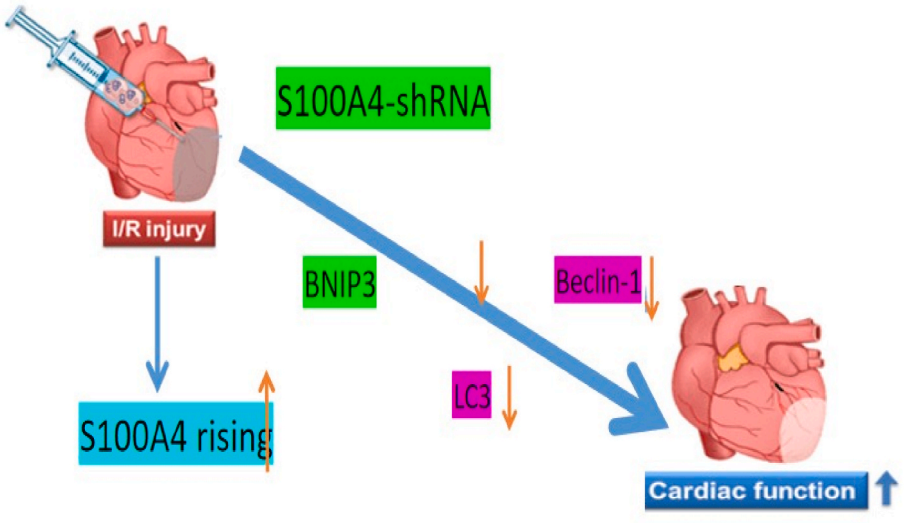

Fig. 6. S100A4-shRNA inhibits autophagy and improves cardiac function.

ferroptosis-related mechanisms. Exploring the crosstalk among S100A4, ferroptosis, and autophagy will be an important focus of our future work.

5. Conclusion

S100A4 experiences up-regulation during MIRI, orchestrating autophagy through the BNIP3 pathway, thereby intricately engaging in the aftermath of reperfusion injury subsequent to myocardial infarction. Through the inhibition of autophagy and the mitigation of inflammatory responses, S100A4-shRNA acts as a safeguard, shielding the heart against the deleterious effects of IRI (Fig. 6).

CRediT authorship contribution statement

Guangwei Huang: Writing – review & editing. **Qing Huang:** Data curation. **Chenrui Mou:** Methodology. **Anna Duan:** Methodology. **Fujiao He:** Software. **Hailong Dai:** Writing – original draft.

Data availability

All data, models, and code genemiceed or utilized during the study are available upon request from the corresponding author.

Code availability

Not applicable.

Ethics approval and consent to participate

Ethics approval and participant assent The authors are responsible for all aspects of the work, including ensuring that any queries regarding the accuracy or integrity of any portion of the work are investigated and resolved appropriately. Animal experiments were approved by the Animal Experimentation Committee of the Institutional Review Board of Anshun city people's hospital and conducted in accordance with the Anshun city people's hospital and Guizhou medical university's guidelines for the care and use of animals. The investigation was conducted in accordance with the 2013 version of the Declaration of Helsinki.

Consent for publication

Not applicable.

Funding

This work was mainly supported by the Anshun City Science and Technology Plan Project (Anshun Science [2023] No. 09), and the Science and Technology Foundation of Health commission of Guizhou Province (Grant No. gzwkj2022-317).

Declaration of competing interest

There are no conflicts of interest.

References

[1] M.J. Domanski, V. Fuster, F. Diaz-Mitoma, et al., Next steps in primary prevention of coronary heart disease: rationale for and design of the ECAD trial, J. Am. Coll. Cardiol. 66 (16) (2015) 1828–1836.
[2] A. Sato, Arrhythmias after acute myocardial infarction, Jpn. J. Clin. Immunol. 74 (Suppl 6) (2016) 145–149.
[3] Z. Hu, F. Ju, L. Du, et al., Empagliflozin protects the heart against ischemia/reperfusion-induced sudden cardiac death, BioMed Central (1) (2021).
[4] E. Gonca, Comparison of thiopental and ketamine+xylazine anesthesia in ischemia/reperfusion-induced arrhythmias in rats, Turk. J. Med. Sci. 45 (6) (2015) 1413, 20.
[5] Y. Shimizu, J.P. Lambert, C.K. Nicholson, et al., DJ-1 protects the heart against ischemia-reperfusion injury by regulating mitochondrial fission, J. Mol. Cell Cardiol. 97 (2016) 56–66.
[6] J.S. Kim, Y. Jin, J.J. Lemasters, Reactive oxygen species, but not Ca2+ overloading, trigger pH- and mitochondrial permeability transition-dependent death of adult rat myocytes after ischemia-reperfusion, American Physiological Society (5) (2006).
[7] L. Dong, Z. Shen, H. Chi, et al., Research progress of Chinese medicine in the treatment of myocardial ischemia–reperfusion injury, Am. J. Chin. Med. (2022).
[8] J. Zhao, D.J. Conklin, Y. Guo, et al., Cardiospecific overexpression of ATPGD1 (carnosine synthase) increases histidine dipeptide levels and prevents myocardial ischemia reperfusion injury, J. Am. Heart Assoc. 9 (12) (2020).
[9] R. Song, C. Dasgupta, C. Mulder, et al., MicroRNA-210 controls mitochondrial metabolism and protects heart function in myocardial infarction, Circulation (New York, N. Y.) 145 (15) (2022) 1140–1153.
[10] M. Abate, A. Festa, M. Falco, et al., Mitochondria as playmakers of apoptosis, autophagy and senescence, Semin. Cell Dev. Biol. (2019) 98.
[11] V.P. Sergey, Regulation of autophagy of the heart in ischemia and reperfusion, Apoptosis : an international journal on programmed cell death 28 (1–2) (2023) 55–80.
[12] A. Marianna, Mitochondria as playmakers of apoptosis, autophagy and senescence, Semin. Cell Dev. Biol. 98 (2020) 139–153.
[13] L. Wang, W. Jiang, J. Wang, et al., Puerarin inhibits FUNDC1-mediated mitochondrial autophagy and CSE-induced apoptosis of human bronchial epithelial cells by activating the PI3K/AKT/mTOR signaling pathway, Aging 14 (3) (2022) 1253–1264.
[14] J.M. Boyd, S. Malstrom, T. Subramanian, et al., Adenovirus E1B 19 kDa and Bcl-2 proteins interact with a common set of cellular proteins, Cell 79 (2) (1994) 341–351.

[15] A. D'Souza, S.R. Hayman, F. Buadi, et al., The utility of plasma vascular endothelial growth factor levels in the diagnosis and follow-up of patients with POEMS syndrome, Blood 118 (17) (2011) 4663–4665.
[16] J.O. Mudd, D.A. Kass, Tackling heart failure in the twenty-first century, Nature (7181) (2008) 451.
[17] Mikael S, Sawa K, C. S C, et al. S100A4 is upregulated in injured myocardium and promotes growth and survival of cardiac myocytes [J]. Cardiovasc. Res., (1): 40.
[18] L. Wen, C. Zhang, Y. Nong, et al., Mild electrical pulse current stimulation upregulates S100A4 and promotes cardiogenesis in MSC and cardiac myocytes coculture monolayer, Cell Biochem. Biophys. 65 (1) (2013) 43–55.
[19] X.J. Gong, X.Y. Song, H. Wei, et al., Serum S100A4 levels as a novel biomarker for detection of acute Myocardial infarction, PubMed (2015).
[20] L. Qian, Y. Zhang, M. Zhu, et al., Improvements in left ventricular regional and global systolic function following treatment with S100A4-shRNA after myocardial infarction in mice, Quant Imaging Med Surg 9 (6) (2019) 1066–1075.
[21] S. Doroudgar, P. Quijada, M. Konstandin, et al., S100A4 protects the myocardium against ischemic stress, J. Mol. Cell. Cardiol. 100 (2016) 54–63.
[22] L. Qian, J. Hong, Y. Zhang, et al., Downregulation of S100A4 alleviates cardiac fibrosis via wnt/beta -catenin pathway in mice, Cell. Physiol. Biochem. 46 (6) (2018) 2551–2560.
[23] Y. Matsui, H. Takagi, X. Qu, et al., Distinct roles of autophagy in the heart during ischemia and reperfusion: roles of AMP-activated protein kinase and Beclin 1 in mediating autophagy, Circ. Res. 100 (6) (2007) 914–922.
[24] H. He, P. Liu, P. Li, Dexmedetomidine ameliorates cardiac ischemia/reperfusion injury by enhancing autophagy through activation of the AMPK/SIRT3 pathway, Drug Des Devel Ther 17 (2023) 3205–3218.
[25] S. Sciarretta, Y. Maejima, D. Zablocki, et al., The role of autophagy in the heart, Annu. Rev. Physiol. 80 (2018) 1–26.
[26] W. Shen, D. Chen, S. Liu, et al., S100A4 interacts with mutant p53 and affects gastric cancer MKN1 cell autophagy and differentiation, Int. J. Oncol. 47 (6) (2015) 2123–2130.
[27] S. Hou, T. Tian, D. Qi, et al., S100A4 promotes lung tumor development through beta-catenin pathway-mediated autophagy inhibition, Cell Death Dis. 9 (3) (2018) 277.
[28] Y. Wang, G. Gao, Y. Wu, et al., S100A4 silencing facilitates corneal wound healing after alkali burns by promoting autophagy via blocking the PI3K/Akt/mTOR signaling pathway, Investig. Ophthalmol. Vis. Sci. 61 (11) (2020) 19.
[29] C. Liu, Y. Liu, H. Chen, et al., Myocardial Injury: where Inflammation and Autophagy Meet, Burns & Trauma, 2023, p. 11.
[30] X. Wang, Z. Guo, Z. Ding, et al., Inflammation, autophagy, and apoptosis after myocardial infarction, J. Am. Heart Assoc. 7 (9) (2018).
[31] N. D'Ambrosi, M. Milani, S. Apolloni, S100A4 in the physiology and pathology of the central and peripheral nervous system, Cells 10 (4) (2021).
[32] L. Zhuang, Y. Wang, Z. Chen, et al., Global characteristics and dynamics of single immune cells after myocardial infarction, J. Am. Heart Assoc. 11 (24) (2022) e027228.
[33] Matteo Marconi, Ciarlo, et al., Autophagic flux and autophagosome morphogenesis require the participation of sphingolipids, Apoptosis: An international journal on programmed cell death 20 (5) (2015) 645–657.
[34] S.L. Ginn, A.K. Amaya, I.E. Alexander, et al., Gene therapy clinical trials worldwide to 2017: an update, J. Gene Med. 20 (5) (2018) e3015.
[35] X. Hou, T. Zaks, R. Langer, et al., Lipid nanoparticles for mRNA delivery, Nat. Rev. Mater. 6 (12) (2021) 1078–1094.
[36] K.K. Ray, U. Landmesser, L.A. Leiter, et al., Inclisiran in patients at high cardiovascular risk with elevated LDL cholesterol, N. Engl. J. Med. 376 (15) (2017) 1430–1440.
[37] J. Zhao, Y. Wu, S. Liang, et al., Activation of SSAT1/ALOX15 Axis aggravates cerebral ischemia/reperfusion injury via triggering neuronal ferroptosis, Neuroscience: An International Journal under the Editorial Direction of IBRO (485) (2022) 485.
[38] Y. Qin, Y. Qiao, D. Wang, et al., Ferritinophagy and ferroptosis in cardiovascular disease: mechanisms and potential applications, Biomed. Pharmacother. 141 (2021) 111872.
[39] J. Zhao, Y. Wu, S. Liang, et al., Activation of SSAT1/ALOX15 Axis aggravates cerebral ischemia/reperfusion injury via triggering neuronal ferroptosis, Neuroscience 485 (2022) 78–90.